

Beyond the Protein Matrix: Probing Cofactor Variants in a Baeyer–Villiger Oxygenation Reaction

Christian Martinoli,[†] Hanna M. Dudek,[‡] Roberto Orru,^{†,†} Dale E. Edmondson,[§] Marco W. Fraaije,^{‡,*} and Andrea Mattevi^{*,†}

[†]Department of Biology and Biotechnology, University of Pavia, Via Ferrata 9, 27100 Pavia, Italy

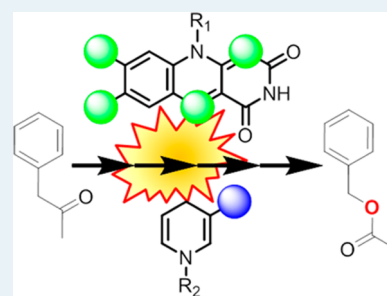
[‡]Molecular Enzymology Group, Groningen Biomolecular Sciences and Biotechnology Institute, University of Groningen, Nijenborgh 4, 9747 AG Groningen, The Netherlands

[§]Departments of Biochemistry and Chemistry, Emory University, 1510 Clifton Road, Atlanta, Georgia 30322, United States

W Web-Enhanced Feature S Supporting Information

ABSTRACT: A general question in biochemistry is the interplay between the chemical properties of cofactors and the surrounding protein matrix. Here, the functions of NADP⁺ and FAD are explored by investigation of a representative monooxygenase reconstituted with chemically modified cofactor analogues. Like pieces of a jigsaw puzzle, the enzyme active site juxtaposes the flavin and nicotinamide rings, harnessing their H-bonding and steric properties to finely construct an oxygen-reacting center that restrains the flavin peroxide intermediate in a catalytically competent orientation. Strikingly, the regio- and stereoselectivities of the reaction are essentially unaffected by cofactor modifications. These observations indicate a remarkable robustness of this complex multicofactor active site, which has implications for enzyme design based on cofactor engineering approaches.

KEYWORDS: cofactors, flavin, nicotinamide, monooxygenation, biocatalysis

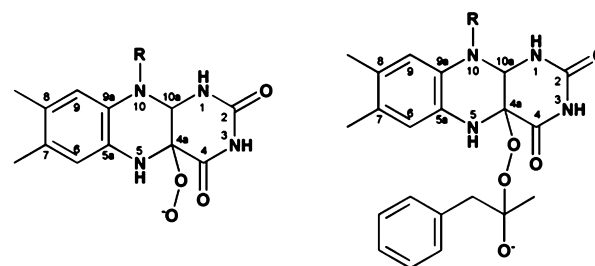


In the fields of biocatalysis and industrial biotechnology, there is a growing interest in the so-called “cofactor engineering”, the idea of tuning the enzyme/cofactor function to make it of interest for green chemistry and industrial processes. By combining suitable host proteins with artificial cofactors, biomimetic, new artificial biocatalysts have been generated.^{1–5} This approach obviously requires a thorough knowledge of the precise functioning of natural cofactors, and from this perspective, it should be noted that the literature on the functional consequences of chemical alterations of enzyme cofactors remains very limited compared with the wealth of studies based on protein engineering.

Along these lines, here, the effects on enzyme catalytic and substrate-specificity properties exerted by chemical modifications of cofactors are explored. As a model system, the FAD-containing and NADPH-dependent phenylacetone monooxygenase (PAMO), which catalyzes the Baeyer–Villiger oxidation of phenylacetone to benzylacetate, is used.⁶ PAMO is a prototype for a large class of flavoenzymes that perform the oxygenation of a variety of compounds, including oxygenation of soft nucleophiles by the drug-metabolizing flavin-dependent monooxygenases, hydroxylation of primary amines by the siderophore-synthesizing ornithine and lysine hydroxylases, and oxygenation of ketones and sulfides by Baeyer–Villiger monooxygenases.^{7,8} Their catalytic reaction starts with the reduction of FAD by NADPH. This is followed by the reaction of the reduced prosthetic flavin group with oxygen to form the crucial flavin (hydro)peroxide. The distal oxygen of this flavin

intermediate is finally inserted into the substrate, this step taking place through a negatively charged tetrahedral intermediate in the case of Baeyer–Villiger monooxygenases such as PAMO (Scheme 1). The fact that NADP(H) and FAD

Scheme 1. Flavin Peroxide (left) and the Postulated Criegee Tetrahedral Intermediate (right)



synergistically act not only as redox cofactors (the textbook function of these molecules) but also as true catalytic elements in oxygen activation and substrate oxygenation makes these enzymes a most insightful test case for our approach.^{9–13}

PAMO was reconstituted with four FAD derivatives, chosen for their varying properties (see Supporting Information (SI)

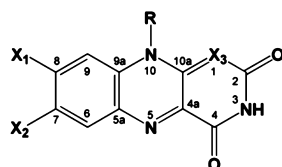
Received: September 20, 2013

Revised: November 1, 2013

Published: November 18, 2013

Table 1. Steady-State Kinetic Parameters

	$V^{[a]}$ (mV)	$k_{cat}(s^{-1})$	$K_M(\mu M)$ NADPH/ APADPH	$k_{cat}(s^{-1})$	$K_M(\mu M)$ phenylacetone
			NADPH	NADPH and phenylacetone	
FAD ^[c]	-208	0.060 ± 0.010	7.90 ± 0.01	2.98 ± 0.01	33.4 ± 2.4
FADrec	-208	0.055 ± 0.012	7.30 ± 0.01	2.48 ± 0.02	43.8 ± 4.4
7-Cl,8-nor-FAD	-128	0.257 ± 0.003	3.87 ± 0.27	0.62 ± 0.02	23.6 ± 3.8
8-Cl-FAD	-152	0.071 ± 0.004	39.27 ± 1.35	1.27 ± 0.06	49.6 ± 8.5
7,8-diCl-FAD	-126	0.025 ± 0.003	n.d. ^[b]	0.48 ± 0.01	50.4 ± 5.0
1-deaza-FAD	-280	0.045 ± 0.003	18.87 ± 2.59	0.14 ± 0.01	11.9 ± 2.5
			APADPH	APADPH and phenylacetone	
FAD	-208	0.080 ± 0.005	<10	0.040 ± 0.005	<10



FAD: $X_1=CH_3$, $X_2=CH_3$, $X_3=N$
 7-Cl, 8-nor-FAD: $X_1=Cl$, $X_2=H$, $X_3=N$
 8-Cl-FAD: $X_1=Cl$, $X_2=CH_3$, $X_3=N$
 7,8-diCl-FAD: $X_1=Cl$, $X_2=Cl$, $X_3=N$
 1-deaza-FAD: $X_1=CH_3$, $X_2=CH_3$, $X_3=CH$

^aThe two-electron redox potential for each flavin analogue is indicated in brackets.^{14,15} For reference, the redox potentials of NADPH and APADPH (25 °C, 1 atm, pH 7) are -320 and -250 mV, respectively.¹⁷ ^bThe K_M value could not be determined because of low activity. ^cThe enzyme was also reconstituted with the 5-deazaFAD which, however, was unreactive against NADPH, as described in SI Figure S3.

and Methods; Figure S1–S3; Table 1).^{14–17} Three of them bear one or two electron-withdrawing chlorine substituents on the flavin dimethylbenzene ring, which results in increased redox potentials. The fourth cofactor analogue is 1-deazaflavin that is modified by replacing nitrogen with carbon on the functionally crucial electron-conjugating N1 position. We first probed the reconstituted enzymes for their NADPH oxidase activity, which arises from the decay (turnover number of $\sim 1 \text{ min}^{-1}$ in the FAD-bound PAMO) of the flavin peroxide to H_2O_2 .⁹ This slow activity turned out to be retained by all reconstituted enzymes. Only the 7-Cl,8-nor-FAD enzyme exhibited a somewhat higher rate, which is in agreement with preliminary studies on cyclohexanone monooxygenase, another enzyme of this class.¹⁶ It is also observed that the modified flavins have small effects on the K_M values for NADPH, despite the fact that the bound nicotinamide stacks above the isoalloxazine moiety of the flavin cofactor, as shown by crystallographic studies (Figure 1).

The next question addressed is if and to what extent flavin modifications can affect the Baeyer–Villiger activity (Table 1).

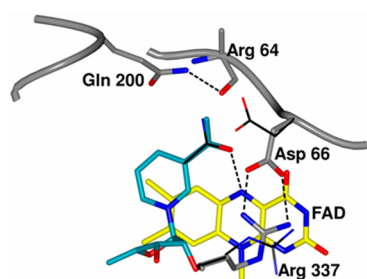


Figure 1. Active site conformation of dithionite-reduced PAMO bound to acetylpyridine adenine dinucleotide (APADP⁺) (this study; PDB: 4C74). Carbons are in gray (protein), yellow (FAD), and cyan (APADP⁺). H bonds are shown as dashed lines. The orientation of the acetyl group of APADP⁺ was assigned on the basis of the H-bonding environment. The carbonyl oxygen of APADP⁺ forms a H bond with the protonated N5 of the reduced FAD. The same H bond is present in the reduced-NADP⁺ enzyme complex. The side chains of Asp66 and Arg337 and the nicotinamide ring of the reduced PAMO–NADP⁺ complex (PDB: 2YLS) are shown as thin lines with carbons in black.

All chlorinated FAD analogues were found to support catalytic monooxygenation at rates that are only 2–5-fold slower than those measured with FAD. This observation is in agreement with the notion that the electronic effects exerted by these electron-withdrawing substituents should favor the deprotonated form of the peroxo intermediate, which is thought to be competent in Baeyer–Villiger oxidation of the substrate (Scheme 1).¹² A significantly lower rate was observed with 1-deazaflavin, which is ~ 20 -fold slower than the natural enzyme, nevertheless displaying considerable substrate conversion (Table 2). We also investigated the effects on the selectivity of the enzyme in the Baeyer–Villiger reaction, an important issue because the biocatalytic potential of Baeyer–Villiger enzymes primarily arises from their regio- and stereoselectivity. Racemic bicyclo[3.2.0]hept-2-en-6-one was used as a test substrate, whose Baeyer–Villiger oxidation can generate four stereo- and regiodivergent products (Table 2 and SI Figure S4).¹⁸ PAMO was previously shown to preferentially (but not exclusively) produce the normal lactone, favoring the (1*R*,5*S*)-enantiomer as a substrate.¹⁹ Strikingly, such a pattern is virtually unchanged with the studied flavin analogues. Retention of stereoselectivity was confirmed by the analysis of thioanisole sulfoxidation, another reaction catalyzed by Baeyer–Villiger monooxygenases (Table 2).²⁰ Collectively, these data outline a remarkable catalytic robustness of the enzyme-bound flavins in terms of retention of the reactivity with NADPH and formation of the flavin peroxide, although the reaction might be limited by different reaction steps (e.g., NADP⁺ release, flavin reduction, or reoxidation), depending on the cofactor analogue. Likewise, the lack of strong effects on the regio- and stereoselectivities implies that the flavin does not provide any specific anchoring point controlling substrate orientation (e.g., H bonds) but, rather, represents a featureless surface that shapes the active site and establishes nonspecific van der Waals interactions with the substrate (Figures 1–2).

A further point of investigation was the sensitivity to chemical modifications of NADPH, the other cofactor necessary for the reaction. We used an acetylpyridine analogue (APADPH) in which the amide group of the nicotinamide moiety is replaced by an acetyl group. The use of APADPH resulted in a relatively slow oxidase activity similar to that

Table 2. Enantioselectivity of the Conversion of Bicyclo[3.2.0]hept-2-en-6-one and Thioanisole Using FAD and NADPH Analogues^a

cofactors	bicyclo[3.2.0]hept-2-en-6-one				thioanisole	
	conversion (%) ^b	normal/abnormal	ee (%) normal	ee (%) abnormal	conversion (%) ^c	ee (%)
FAD + NADPH	44	71:29	94	74	33	24
7-Cl,8-nor-FAD + NADPH	48	70:30	76	68	34	40
8-Cl-FAD + NADPH	46	70:30	92	72	38	36
1-deaza-FAD + NADPH	32	75:25	95	88	11	23
FAD + APADPH	8	72:28	45	77	40	15

^aAt first, PAMO converts the (1*R*,5*S*)-ketone and produces an excess of the “normal” lactone with ee in favor of the (1*S*,5*R*)-enantiomers for both lactones (SI Figure S4). As the (1*R*,5*S*)-substrate is depleted, the (1*S*,5*R*)-ketone is also converted, yielding mainly the abnormal lactone. Therefore, the ratio of the normal to the abnormal lactones and the enantiomeric excess of the abnormal product are conversion-dependent. However, in our experiments, reactions were stopped before 50% of conversion was reached, which allows fair comparison. The percent enantiomeric excesses (ee) are reported in favor of the (1*S*,5*R*) products. The 7,8-diCl-FAD reconstituted enzyme exhibited a tendency to precipitate in the assay conditions (see SI), and therefore, no reliable observations could be made. ^bAverage of duplicate experiments. ^cEstimated on the basis of the peak area of the product.

measured for NADPH (Table 1). However, the addition of phenylacetone did not result in a burst of APADPH consumption. Instead, phenylacetone triggered an even slower conversion of APADPH, indicating that phenylacetone conversion was, at best, very inefficient. Consistently, we found that the reaction is only 30% coupled, implying that flavin reoxidation occurs mostly through the abortive generation of hydrogen peroxide rather than through substrate oxygenation (either phenylacetone or thioanisole; SI Table S1). This is in sharp contrast with NADPH, which gives 100% coupling (i.e., for each molecule of oxidized NADPH, a substrate molecule is converted). Presteady state kinetics underpinned these observations, showing that with APADPH as an electron donor, there is a 20-fold decrease in the rate of formation of the flavin peroxide, which decays 100-fold more rapidly (SI Table S2). Furthermore, these rates are unaffected by the presence of phenylacetone. Thus, the high uncoupling results from the combination of decreased efficiencies in two critical catalytic steps, stable flavin-peroxide formation, and substrate oxygenation. Such a clear demonstration of the role of the bound pyridine dinucleotide in fine-tuning the reactivity with oxygen prompted us to investigate the crystal structures of both oxidized and reduced PAMO bound to APADP⁺ (SI Figure S5, Table S3). In both cases, the binding of APADP⁺ is virtually identical to that of NADP⁺ (Figure 1 and SI S6); however, the presence of the less polar acetyl group induces a conformational change of Asp66, which is now oriented toward the active site with its carboxylate group positioned in direct contact with the flavin C4a atom. These features were confirmed by determining the structure of a PAMO mutant (SI Figure S7) and finely correlate with the kinetic properties of the APADPH-reduced enzyme: (i) the proximity of negative charges (e.g., Asp66) is known to generally decrease the reactivity of the reduced flavin with oxygen through destabilization of the proposed radical pair intermediate consisting of a complex of the superoxide anion and neutral flavin radical,²¹ and (ii) the relocated Asp66 can hamper stabilization of the oxygen-adduct on the C4a atom. This conformation of Asp66 and the associated alteration of the H-bonding environment around the oxygen-reacting and substrate-binding site can also possibly explain the observed slight changes in the enantioselectivity of the reaction with APADPH (Table 2).

These findings demonstrate that even subtle alterations in the configuration of the oxygen-reacting center can drastically

affect the outcome of the oxygen reaction. The comparative analysis of the three-dimensional structures of members of the class of Baeyer–Villiger and similar enzymes^{22–27} shows that the shape of the active site is such that the oxygen molecule is steered toward the flavin to promote an approach that is suited for the formation of the oxygen-covalent adduct (Figure 2).²⁸ In more detail, inspection of the active site geometries of these enzymes consistently indicates that oxygen is seemingly forced to approach the cofactor C4a–N5 locus from the flavin ring face (i.e., side-on) rather than the edge (edge-on). This is the geometry expected to support the formation of the flavin peroxide, whose oxygen atoms protrude out the cofactor plane. Once the flavin peroxide is formed, the distal oxygen of the intermediate is restrained to be oriented toward the ribityl chain, away from the flavin N5 atom. This location (at the very rear of the active site) protects the intermediate from decay, which is primarily triggered by protonation of the peroxide proximal oxygen by either water or protein groups, as shown by computational studies.²⁹ The hydrogen-bonding and steric properties of the NADP⁺ amide and ribose are the pillars that hold up this active site configuration through their interactions with the flavin N5 atom and nearby side chains. In this context, it is instructive to compare this mechanistic strategy with that of aromatic hydroxylases, a class that is distinct from that of PAMO.³⁰ In these flavoenzymes, the flavin peroxide forms only after (rather than before, as in PAMO) binding of the aromatic substrate, which affords a highly coupled hydroxylation, despite the fact that the intermediate has limited stability (a half-life of milliseconds rather than minutes). This difference reflects the opposite geometry of the oxygen attack compared with PAMO and related monooxygenases: the protein environment of aromatic hydroxylases forces the peroxide distal oxygen to be oriented toward the flavin N5 (compare Figure 2 and SI Figure S8).³¹ This orientation makes the intermediate oxygens accessible to protonation, specifically including the possibility of a water-mediated proton transfer from N5, which would inevitably cause H₂O₂ elimination.³²

Thus, PAMO (and generally, the related flavoenzyme class) features the distinctive ability to optimally harness the steric and hydrogen-bonding properties of NADP⁺ to both enhance the reaction of the reduced flavin with oxygen and, even more crucial, most effectively prevent the decay of the labile oxygen-activating intermediate that underlies substrate oxygenation. The uncovered delicate roles of the nicotinamide and flavin

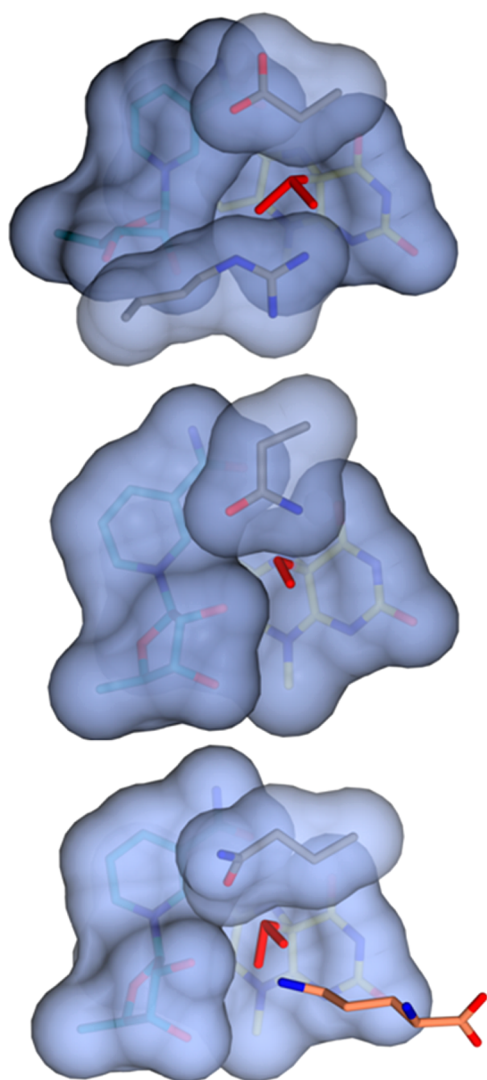


Figure 2. Comparison of Baeyer–Villiger enzyme three-dimensional structures^{22–27} shows that they all feature very similar, if not identical, oxygen-reacting centers formed by the juxtaposition of the nicotinamide–ribose of NADP⁺ and the flavin (with reference to the so-called “closed” conformation,²³ which is thought to represent the protein state reacting with O₂). Such a conservation is particularly significant, given the limited (<30%) sequence identities and the high diversity of the substrates used by these enzymes. This is outlined by modeling the flavin peroxide intermediate in three exemplifying NADP-bound enzyme structures analyzed in their reduced state (i.e., the state that reacts with O₂): PAMO (top; 2YLS), bacterial FMO (middle; 2VQB), and ornithine hydroxylase SidA (bottom; 4B65). The geometry of the flavin peroxide was modeled by using as reference the three-dimensional structures of a flavin hydroxide bound to pyranose oxidase³³ and of a covalent C4a-inhibitor adduct in monoamine oxidase B.³⁴ The van der Waals surfaces of the flavin ring, NADP⁺, and side chains interacting with the C4a-OOH atoms (Asp66 and Arg337 in PAMO, Asn78 in FMO, Gln102 in SidA) are depicted. The drawing highlights the conformation (FMO) or narrow range of conformations (PAMO, SidA) permitted for the intermediate distal oxygen within the niche formed by the nicotinamide–ribose moiety and adjacent side chains. The substrate-binding site is located on the right-hand side of the intermediate oxygens above the pyrimidine ring of the flavin, as outlined by ornithine (carbons in orange) bound to SidA. A clip movie representing the geometry and environment of the flavin peroxide model in PAMO is available in the HTML version of this article on the ACS Web site.

cofactors in enzyme catalysis will be of help in future enzyme redesign efforts that include cofactor engineering.

■ ASSOCIATED CONTENT

■ Supporting Information

Experimental procedures for chemical syntheses, enzyme purification and reconstitution, kinetic studies, and X-ray analyses. This material is available free of charge via the Internet at <http://pubs.acs.org>.

■ Web-Enhanced Feature

A movie clip representing the geometry of the flavin peroxide intermediate in PAMO is available in the HTML version of this article.

■ AUTHOR INFORMATION

■ Corresponding Author

*E-mail: andrea.mattevi@unipv.it, m.w.fraaije@rug.nl.

■ Present Address

†Dr. Roberto Orru is currently at Departments of Biochemistry and Chemistry, Emory University, Atlanta, GA 30322, USA.

■ Notes

The authors declare no competing financial interest.

■ ACKNOWLEDGMENTS

Financial support from the Fondazione Cariplo (No. 2008.3148), NIH grant GM 29433, and the EU (EU-FP7 OXYGREEN project, Grant No. 212281) is gratefully acknowledged. We acknowledge the European Synchrotron Radiation Facility and the Swiss Light Source for beam time and excellent support during X-ray data collection.

■ REFERENCES

- (1) Campbell, E.; Meredith, M.; Minter, S. D.; Banta, S. *Chem. Commun.* **2012**, *48*, 1898–900.
- (2) Paul, C. E.; Gargiulo, S.; Opperman, D. J.; Lavandera, I.; Gotor-Fernández, V.; Gotor, V.; Taglieber, A.; Arends, I. W.; Hollmann, F. *Org. Lett.* **2013**, *15*, 180–183.
- (3) Köhler, V.; Wilson, Y. M.; Dürrenberger, M.; Ghislieri, D.; Churakova, E.; Quinto, T.; Knörr, L.; Häussinger, D.; Hollmann, F.; Turner, N. J.; Ward, T. R. *Nat. Chem.* **2013**, *5*, 93–99.
- (4) de Gonzalo, G.; Smit, C.; Jin, J.; Minnaard, A. J.; Fraaije, M. W. *Chem. Commun.* **2011**, *47*, 11050–11052.
- (5) Zilly, D. E.; Taglieber, A.; Schulz, F.; Hollmann, F.; Reetz, M. T. *Chem. Commun.* **2009**, *46*, 7152–7154.
- (6) de Gonzalo, G.; Mihovilovic, M. D.; Fraaije, M. W. *ChemBioChem* **2010**, *11*, 2208–2231.
- (7) Leisch, H.; Morley, K.; Lau, P. C. *Chem. Rev.* **2011**, *111*, 4165–222.
- (8) van Berkel, W. J.; Kamerbeek, N. M.; Fraaije, M. W. *J. Biotechnol.* **2006**, *124*, 670–689.
- (9) Torres Pazmiño, D. E.; Baas, B. J.; Janssen, D. B.; Fraaije, M. W. *Biochemistry* **2008**, *47*, 4082–4093.
- (10) Alfieri, A.; Malito, E.; Orru, R.; Fraaije, M. W.; Mattevi, A. *Proc. Natl. Acad. Sci. U.S.A.* **2008**, *105*, 6572–6577.
- (11) Orru, R.; Dudek, H. M.; Martinoli, C.; Torres Pazmiño, D. E.; Royant, A.; Weik, M.; Fraaije, M. W.; Mattevi, A. *J. Biol. Chem.* **2011**, *286*, 29284–29291.
- (12) Sheng, D.; Ballou, D. P.; Massey, V. *Biochemistry* **2001**, *40*, 11156–11167.
- (13) Polyak, I.; Reetz, M. T.; Thiel, W. *J. Am. Chem. Soc.* **2012**, *134*, 2732–2741.
- (14) Edmondson, D. E.; Ghisla, S. In *Flavin and Flavoproteins*; Ghisla, S., Kroneck, P., Macheroux, P., Sund, H., Eds.; Weber: Berlin, 1999; pp 71–76.
- (15) Ghisla, S.; Massey, V. *Biochem. J.* **1986**, *239*, 1–12.

- (16) Ryerson, C. C.; Ballou, D. P.; Walsh, C. *Biochemistry* **1982**, *21*, 2644–2655.
- (17) Ciotti, M. M.; Kaplan, N. O.; Stolzenbach, F. E. *J. Biol. Chem.* **1956**, *221*, 833–844.
- (18) Roberts, S. M.; Wan, P. W. H. *J. Mol. Catal. B: Enzym.* **1998**, *4*, 111–136.
- (19) Dudek, H. M.; de Gonzalo, G.; Pazmiño, D. E.; Stepniak, P.; Wyrwicz, L. S.; Rychlewski, L.; Fraaije, M. W. *Appl. Environ. Microbiol.* **2011**, *77*, 5730–5738.
- (20) Colonna, S.; Gaggero, N.; Pasta, P.; Ottolina, G. *Chem. Commun.* **1996**, *20*, 2303–2307.
- (21) Gadda, G. *Biochemistry* **2012**, *51*, 2662–2669.
- (22) Franceschini, S.; van Beek, H. L.; Pennetta, A.; Martinoli, C.; Fraaije, M. W.; Mattevi, A. *J. Biol. Chem.* **2012**, *287*, 22626–22634.
- (23) Mirza, I. A.; Yachnin, B. J.; Wang, S.; Grosse, S.; Bergeron, H.; Imura, A.; Iwaki, H.; Hasegawa, Y.; Lau, P. C.; Berghuis, A. M. *J. Am. Chem. Soc.* **2009**, *131*, 8848–54.
- (24) Leisch, H.; Shi, R.; Grosse, S.; Morley, K.; Bergeron, H.; Cygler, M.; Iwaki, H.; Hasegawa, Y.; Lau, P. C. *Appl. Environ. Microbiol.* **2012**, *78*, 2200–22012.
- (25) Orru, R.; Pazmiño, D. E.; Fraaije, M. W.; Mattevi, A. *J. Biol. Chem.* **2010**, *285*, 35021–25028.
- (26) Mayfield, J. A.; Frederick, R. E.; Streit, B. R.; Wencewicz, T. A.; Ballou, D. P.; DuBois, J. L. *J. Biol. Chem.* **2010**, *285*, 30375–30388.
- (27) Olucha, J.; Meneely, K. M.; Chilton, A. S.; Lamb, A. L. *J. Biol. Chem.* **2011**, *286*, 31789–31798.
- (28) Chaiyen, P.; Fraaije, M. W.; Mattevi, A. *Trends Biochem. Sci.* **2012**, *37*, 373–380.
- (29) Bach, R. D.; Mattevi, A. *J. Org. Chem.* **2013**, *78*, 8585–8593.
- (30) Entsch, B.; van Berkel, W. J. *FASEB J.* **1995**, *9*, 476–483.
- (31) Schreuder, H. A.; Hol, W. G.; Drenth, J. *Biochemistry* **1990**, *29*, 3101–3108.
- (32) Sucharitakul, J.; Wongnate, T.; Chaiyen, P. *Biochemistry* **2010**, *49*, 3753–3765.
- (33) Tan, T. C.; Spadiut, O.; Wongnate, T.; Sucharitakul, J.; Krondorfer, I.; Sygmund, C.; Haltrich, D.; Chaiyen, P.; Peterbauer, C. K.; Divne, C. *PLoS One.* **2013**, *8*, e53567.
- (34) Binda, C.; Li, M.; Hubalek, F.; Restelli, N.; Edmondson, D. E.; Mattevi, A. *Proc. Natl. Acad. Sci. U.S.A.* **2003**, *100*, 9750–9755.

■ NOTE ADDED AFTER ASAP PUBLICATION

After this paper was published ASAP on November 22, 2013, a correction was made to the funding information in the Acknowledgment. The corrected version was reposted on November 26, 2013